

The qualitative agreement is quite evident and similar to that obtained for other deformed nuclei. One should not, however, look for a quantitative agreement since the above comparison does not take into account the pairing effect which determines the extent to which a particular single-particle state is filled or empty.

The experimental data on other properties, when available, will certainly be of a great interest in further establishing the validity of the model. According to these calculations the quadrupole moment for the ground state should have a value

$$Q_s = [3K^2 - I(I+1)] / (I+1)(2I+3) \\ \times 1.25ZA^{2/3}\delta(1+0.5\delta+\dots) \times 10^{-26} \text{ cm}^2 \quad (9) \\ = (0.15 \pm 0.05) \times 10^{-24} \text{ cm}^2$$

for  $\delta = 0.14 \pm 0.02$ . Also the band structure proposed in Fig. 4 leads to interband and intraband transition rate estimates which can be easily checked experimentally. For instance, the  $E2$  decay of the 1026-keV  $\frac{7}{2}^-$  state can either go to 728-keV  $\frac{5}{2}^-$  state or to the

$\frac{3}{2}^-$  ground state, in one case with  $\Delta K = -1$  and in the other case with no change in  $K$ , and thus with distinguishable transition rates. Similar selection-rule features will appear in other transition rates and mixing ratios as well. Also it may be noted that both the  $K = \frac{1}{2}$  bands are built on hole states whereas the excited  $K = \frac{3}{2}$  and  $K = \frac{5}{2}$  bands are built on particle states, and such intraband transitions are not favored.

The experimental information on the spin-parity assignments suggested here and on the various electromagnetic moments, transition rates, mixing ratios, etc., will be necessary to assess properly the merits of this approach.

#### ACKNOWLEDGMENTS

The author is grateful to D. A. Hutcheon for help with the calculations which were carried out at the University of Alberta computing centre. The hospitality of the Institute for Nuclear Study, University of Tokyo (under financial support from the Japan Council for Promotion of Science) during the final phases of this work is gratefully acknowledged.

### Excitation Functions for Radioactive Nuclides Produced by Deuteron-Induced Reactions in Iron\*

J. W. CLARK,† C. B. FULMER, AND I. R. WILLIAMS‡

*Oak Ridge National Laboratory, Oak Ridge, Tennessee 37830*

(Received 25 November 1968)

Cross sections were measured for the production of radioactive nuclides by deuteron-induced reactions in natural iron at bombarding energies below 40 MeV. Deuteron beams of the Oak Ridge isochronous cyclotron were used to bombard stacked iron foils.  $\gamma$  spectra of individual foils were measured with a Ge(Li) spectrometer. Radioactivities with half-lives greater than 20 min were measured. Excitation functions were obtained for  $^{56}\text{Co}$ ,  $^{56}\text{Co}$ ,  $^{57}\text{Co}$ ,  $^{58}\text{Co}$ ,  $^{52}\text{Mn}$ ,  $^{54}\text{Mn}$ ,  $^{54}\text{Mn}^m$ , and  $^{51}\text{Cr}$ . Cross sections predicted by a compound-nucleus evaporation theory are in reasonable agreement with the experimental results.

#### INTRODUCTION

**E**XCITATION functions for the production of radioactive nuclides by charged-particle-induced reactions are of interest as part of a continuing study of the residual radiation that is produced in the vicinity of particle accelerators.<sup>1-4</sup> Excitation function data

can also contribute to an understanding of the reaction mechanisms involved. Only a few excitation functions for production of radioactive nuclides by deuteron induced reactions in iron<sup>5,6</sup> have been reported. The Ge(Li)  $\gamma$  spectrometer,<sup>7-9</sup> with an energy resolution of a few keV, makes the measurements of such excitation functions relatively simple.

\* Research sponsored by the U.S. Atomic Energy Commission under contract with the Union Carbide Corporation.

† 1968 Oak Ridge Associated Universities student trainee from Gonzaga University, Spokane, Washington.

‡ 1968 Oak Ridge Associated Universities Research Participant from Knoxville College, Knoxville, Tennessee.

<sup>1</sup> C. B. Fulmer, K. S. Toth, and M. Barbier, *Nucl. Instr. Methods* **31**, 45 (1964).

<sup>2</sup> K. S. Toth, C. B. Fulmer, and M. Barbier, *Nucl. Instr. Methods* **42**, 128 (1966).

<sup>3</sup> C. B. Fulmer, K. S. Toth, and M. Barbier, *IEEE Trans. Nucl. Sci.* **12**, 673 (1965).

<sup>4</sup> C. B. Fulmer, I. R. Williams, and J. B. Ball, *IEEE Trans. Nucl. Sci.* **14**, 977 (1967).

<sup>5</sup> N. A. Vlasov, S. P. Kalinin, A. A. Ogloblin, V. M. Pankramov, V. P. Rudakov, I. N. Serikov, and V. A. Sidorov, *At. Energ. (USSR)* **2**, 169 (1957) [English transl.: *Soviet J. At. Energ.* **2**, 189 (1957)].

<sup>6</sup> W. H. Burgus, G. A. Cowan, J. W. Haldey, W. Hess, T. Shull, M. L. Stevenson, and H. F. York, *Phys. Rev.* **95**, 750 (1954).

<sup>7</sup> G. T. Ewan and A. J. Tavendale, *Can. J. Phys.* **42**, 2286 (1964).

<sup>8</sup> W. L. Hansen and B. V. Jarrett, *Nucl. Instr. Methods* **31**, 301 (1964).

<sup>9</sup> R. J. Fox, I. R. Williams, and K. S. Toth, *Nucl. Instr. Methods* **35**, 331 (1965).

In the work reported here cross sections were measured for production of radionuclides from reactions induced by  $\leq 40$ -MeV deuterons incident on natural iron.

### EXPERIMENTAL PROCEDURE

Two stacks of iron foils were bombarded with deuterons at the Oak Ridge isochronous cyclotron. The foils were 2 in. square and 0.005 or 0.002 in. thick, stacked separately. The total thickness of the stacks was sufficient to stop beams of  $\sim 40$ - and  $\sim 20$ -MeV deuterons, respectively. The beams were focused in  $\sim 0.5$  in. diam spots in the center of the targets. The target holder was electrically insulated and served as a Faraday cup to record, with an accuracy of  $\pm 1\%$ , the total charge deposited by the deuterons. Integrated beams of  $\sim 10^{14}$  deuterons were used.

After a few minutes of bombardment the  $\gamma$  spectra of each foil were measured with a 6-cm<sup>3</sup> Ge(Li) spectrometer.<sup>9</sup> A Tennelec (TC 120) field-effect-transistor preamplifier and Tennelec (TC 200) linear amplifier were used. The energy resolution was 7 keV full width at half maximum (FWHM) at 570 keV. The calibration of the spectrometer with a <sup>207</sup>Bi source of known strength permitted measurement of both the  $\gamma$  energy and the intensity of the peak. The pulse-height spectra were analyzed with a 20 000-channel Victoreen pulse-height analyzer used in a 20 $\times$ 1000 mode. The data were transferred directly to an SEL 840A computer for which a program was available to graph the spectra with the printer.

Each spectrum plot and data list was used to measure the number of counts per unit time in the total effects (mostly photoelectric) peaks. All peaks, except the 511-keV positron annihilation peak, were identified as due to prominent  $\gamma$  rays from the various isotopes. The absolute detector efficiency and decay scheme data<sup>10</sup> were used to convert peak intensity to source strength of each radioisotope. These data together with foil thickness and beam current measurements were used to calculate production cross sections for all nuclides observed in each foil.

The energy of deuterons after they had traversed half the thickness of each target foil was computed from range-energy tables.<sup>11</sup> The uncertainty of deuteron energy for each datum point is due to the energy spread of the incident beam (which was 0.2%) and to energy-loss straggling. The latter was obtained from tabulated Vavilov<sup>12</sup> distributions. These tables do not give the straggling for deuterons, so the values used were those for protons having the same velocity as the deuterons.

<sup>10</sup> C. M. Lederer, J. M. Hollander, and I. Perlman, *Table of Isotopes* (John Wiley & Sons, Inc., New York, 1967), 6th ed.

<sup>11</sup>  $dE/dx$  and Range Energy Computer Program, H. Bischsel, Tech. Report No. 3, Physics Department, University of Southern California, 1961 (unpublished).

<sup>12</sup> S. M. Seltzer and M. J. Berger, Natl. Acad. Sci.—Natl. Res. Coun. Publ. 1133, Nucl. Sci. Series Report No. 39, 1964 (unpublished).

TABLE I. Nuclides identified in the  $\gamma$ -ray spectra. The  $\gamma$  energies and branching ratios (obtained from Ref. 10) used in absolute intensity calculations are listed. All internal-conversion coefficients were assumed to be zero.

Nuclide	Half-life	Radiation (keV)	Branching ratio
<sup>51</sup> Cr	27.8 days	320	9%
		744	82%
		935	84%
<sup>52</sup> Mn	5.7 days	1434	100%
		1434	100%
		1434	100%
<sup>54</sup> Mn	303 days	835	100%
<sup>56</sup> Mn	3.576 h	847	99%
		1811	29%
		1811	29%
<sup>55</sup> Co	18.2 h	480	12%
		930	80%
		1410	13%
<sup>56</sup> Co	77 days	847	100%
		1038	12.4%
		1239	66%
		1760	15.6%
<sup>57</sup> Co	270 days	122	85%
<sup>58</sup> Co	71.3 days	810	100%

The straggling for a particular foil depends upon the depth of the foil in the stack. For incident monoenergetic 39-MeV deuterons the calculated energy-loss straggling was 0.13 MeV FWHM for the first foil and 0.54 MeV in the foil in which the deuterons had been slowed to 16 MeV. It was for this reason that a second bombardment was made at 20 MeV.

The foils were sufficiently thin that most measurements were made at less than 10% increments in deuteron energy. Spectra were measured at time intervals suitable for identifying the nuclides by half-life as well as  $\gamma$  energy.

### RESULTS AND DISCUSSION

The nuclides identified in this work are listed in Table I, along with the half-lives and characteristic radiation, by which the nuclides were identified. The  $Q$  values (calculated from the data of Ref. 13) for the nuclear reactions of the lowest threshold energies that can produce the nuclides are listed in Table II.

Excitation functions previously measured<sup>5,6</sup> by other workers are graphed in Fig. 1.

The excitation functions measured in the present work are shown in Figs. 2 and 3. Each curve is identified by the nuclide whose decay radiation was measured, but may include contributions from shorter-

<sup>13</sup> J. H. E. Mattauch, W. Thiele, and A. H. Wapstra, Nucl. Phys. **67**, 1 (1965).

TABLE II. Reactions that involve the largest numerical  $Q$  value to produce the radionuclide identified. The  $Q$  values are calculated from the 1964 Atomic Mass Table of Mattauch *et al.*, [Nucl. Phys. 67, 1 (1965)]; they are expressed in laboratory coordinates. The target was natural iron:  $^{54}\text{Fe}$  (5.8%),  $^{56}\text{Fe}$  (91.7%),  $^{57}\text{Fe}$  (2.2%).

Reaction	$Q$ value (MeV)
$^{57}\text{Fe}(d, \alpha 3n)^{52}\text{Mn}$	-23.8
$^{56}\text{Fe}(d, \alpha 2n)^{52}\text{Mn}$	-15.9
$^{54}\text{Fe}(d, \alpha)^{52}\text{Mn}$	+5.4
$^{57}\text{Fe}(d, \alpha n)^{54}\text{Mn}$	-2.1
$^{56}\text{Fe}(d, \alpha)^{54}\text{Mn}$	+5.9
$^{54}\text{Fe}(d, 2p)^{54}\text{Mn}$	-2.2
$^{57}\text{Fe}(d, dp)^{56}\text{Mn}$	-10.9
$^{56}\text{Fe}(d, 2p)^{56}\text{Mn}$	-5.3
$^{56}\text{Fe}(d, 3n)^{55}\text{Co}$	-18.3
$^{54}\text{Fe}(d, n)^{55}\text{Co}$	+2.9
$^{57}\text{Fe}(d, 3n)^{56}\text{Co}$	-15.7
$^{56}\text{Fe}(d, 2n)^{56}\text{Co}$	-7.9
$^{54}\text{Fe}(d, \gamma)^{56}\text{Co}$	+13.4
$^{57}\text{Fe}(d, 2n)^{57}\text{Co}$	-4.0
$^{56}\text{Fe}(d, n)^{57}\text{Co}$	+3.9
$^{57}\text{Fe}(d, n)^{58}\text{Co}$	+4.9
$^{56}\text{Fe}(d, \gamma)^{58}\text{Co}$	+12.8
$^{56}\text{Fe}(d, \alpha 3n)^{51}\text{Mn}$	-26.8
$^{54}\text{Fe}(d, \alpha n)^{51}\text{Mn}$	-5.6
$^{56}\text{Fe}(d, \alpha t)^{51}\text{Cr}$	-13.9
$^{54}\text{Fe}(d, \alpha p)^{51}\text{Cr}$	-1.4

lived precursors in a decay chain. For example,  $\text{Fe}(d, x)^{51}\text{Mn} \rightarrow ^{51}\text{Cr} + \beta^+$  would contribute to the measured yield of  $^{51}\text{Cr}$ .  $^{51}\text{Mn}$  was not observed because the decay of that nuclide to  $^{51}\text{Cr}$  by positron emission or electron capture, is almost 100% to the ground state. The half-life of  $^{51}\text{Mn}$  is 45 min while that of  $^{51}\text{Cr}$  is 27.8 days; therefore,  $^{51}\text{Mn}$  produced during bombardment will be detected as  $^{51}\text{Cr}$  in spectra measured several hours or days after bombardment.

Data points are shown for  $^{56}\text{Co}$ : These data are representative of the measurements obtained in this work. The data for the two bombarding energies overlap almost 5 MeV, and good agreement is obtained. Absolute normalization probable errors of  $\pm 30\%$  are assigned to the data. These are due principally to the uncertainty of the absolute photopeak-detection efficiency of the spectrometer and miscellaneous smaller uncertainties. An uncertainty of  $\pm 40\%$  is assigned the absolute normalization of the excitation function for  $^{57}\text{Co}$ . That nuclide was identified by a 122-keV  $\gamma$ .

The measured excitation functions for  $^{52}\text{Mn}$  and  $^{54}\text{Mn}$  (Fig. 2) exhibit a peak, a valley, and a second peak. This is evidence of different reactions contributing to the measured yields as the deuteron energy changes.

For example, production of  $^{52}\text{Mn}$  below  $\sim 23$  MeV is believed to be principally because of  $^{54}\text{Fe}(d, \alpha)$  reactions; above 23 MeV it is principally by means of  $^{56}\text{Fe}(d, \alpha 2n)$  and  $^{56}\text{Fe}(d, 2t)$  reactions. This observation is in agreement with the threshold energies for these reactions (Table II). The double peaked excitation function for production of  $^{55}\text{Co}$  also exhibits contributions from reactions on  $^{54}\text{Fe}$  and  $^{56}\text{Fe}$ , respectively.

Comparison of the excitation functions for production of  $^{55}\text{Co}$ ,  $^{56}\text{Co}$  (Fig. 3), and  $^{52}\text{Mn}$  (Fig. 2) with the previously reported measurements (Fig. 1) shows reasonable agreement with the shapes of the respective curves for the overlapping energy range. In each case, however, the absolute normalization of the present data is larger. The  $^{56}\text{Co}$  yield at 15–20 MeV shown in Fig. 3 is  $\sim 35\%$  larger than the yields reported in Ref. 6 and shown in Fig. 1. If the yield of  $^{55}\text{Co}$  below the minimum of the curve in Fig. 3 is assumed to be produced by  $^{54}\text{Fe}$  reactions the measured cross sections are  $\sim 50\%$  larger than those reported in Ref. 5 and shown in Fig. 1. Similarly, the yield of  $^{52}\text{Mn}$  in the low-energy peak of the curve shown in Fig. 2 is  $\sim 40\%$  larger than that of Ref. 6 (Fig. 1) when a correction is made for the isotopic abundance of  $^{54}\text{Fe}$ . If it is assumed that the low-energy parts of the excitation functions for  $^{52}\text{Mn}$  and  $^{52}\text{Mn}^m$  are both the result of  $^{54}\text{Fe}(d, \alpha)$  reactions, then the cross section for  $^{54}\text{Fe}(d, \alpha)$  at the peak of the excitation function is almost a factor of three larger than the value reported in Ref. 6.

The sum of yields of  $^{52}\text{Mn}$  and  $^{52}\text{Mn}^m$  in the region of peaks between 10 and 15 MeV divided by the isotopic

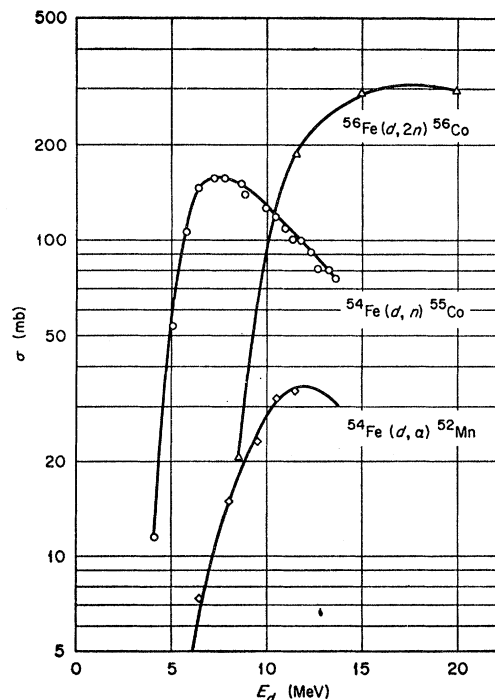


FIG. 1. Excitation functions reported in the literature (Refs. 5 and 6) for deuteron-induced reactions in iron that result in radioactive nuclides.

abundance of  $^{54}\text{Fe}$  is in good agreement with the yield in the same energy region of the  $^{54}\text{Mn}$  excitation function. This suggests that in this energy region the  $^{54}\text{Mn}$  is produced principally by  $^{56}\text{Fe}(d, \alpha)$  and the  $^{52}\text{Mn}$  is produced principally by  $^{54}\text{Fe}(d, \alpha)$  reactions. The  $^{52}\text{Mn}$  and  $^{52}\text{Mn}^m$  curves have the same general shapes. There are some observable differences, however. The peak

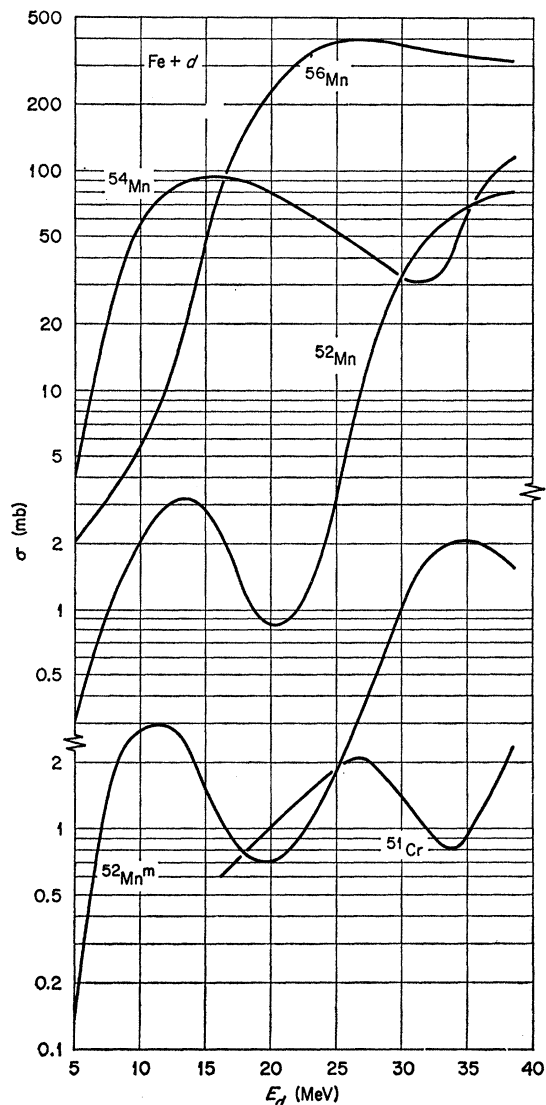


FIG. 2. Excitation functions for production of radioisotopes of Cr and Mn by deuteron-induced reactions in natural iron. Deuteron energies are in laboratory coordinates.

near 12 MeV occurs  $\sim 2$  MeV lower for  $^{52}\text{Mn}^m$  than for  $^{52}\text{Mn}$ . Above 35 MeV, the yield of  $^{52}\text{Mn}^m$  shows a decrease that is not observed in the  $^{52}\text{Mn}$  data.

The curves for  $^{57}\text{Co}$  and  $^{56}\text{Co}$  and the upper part of the curve for  $^{56}\text{Co}$  (Fig. 3) are apparently due principally to  $(d, n)$ ,  $(d, 2n)$ , and  $(d, 3n)$  reactions, respectively, on  $^{56}\text{Fe}$ . The  $^{56}\text{Co}$  curve approaches zero at the  $^{56}\text{Fe}(d, 2n)$  threshold (Table II). The  $Q$  value for  $^{56}\text{Fe}(d, n)^{57}\text{Co}$  is  $+3.9$  MeV. At energies below 5 MeV

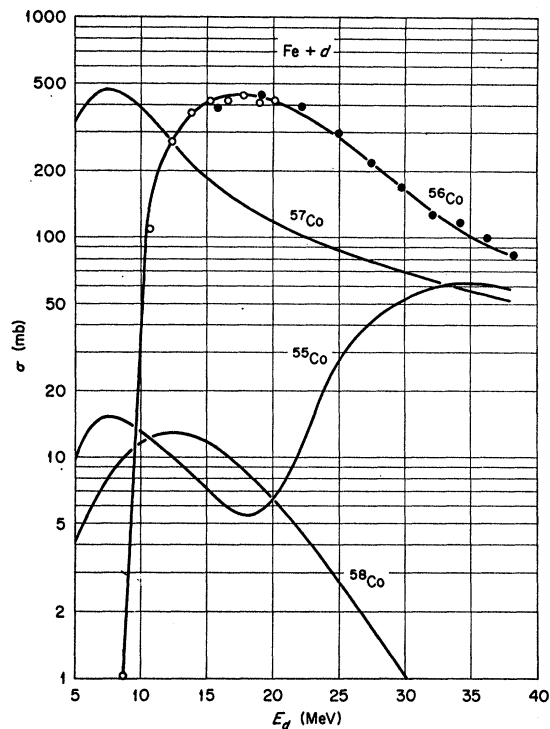


FIG. 3. Excitation functions for production of radioisotopes of Co by deuteron-induced reactions in natural iron. Deuteron energies are in laboratory coordinates. Open circles are data points obtained from a 20-MeV bombardment; full circles are data points obtained from a 40-MeV bombardment.

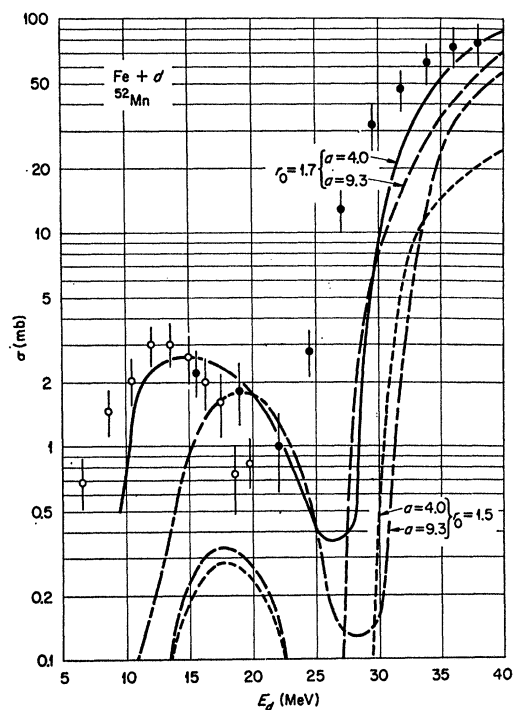


FIG. 4. Calculated excitation functions for production of  $^{52}\text{Mn}$  compared with the experimental data. The curves predicted by the theory (Ref. 14) were obtained by using the parameters indicated. The errors shown for the data points include uncertainties in absolute normalization.

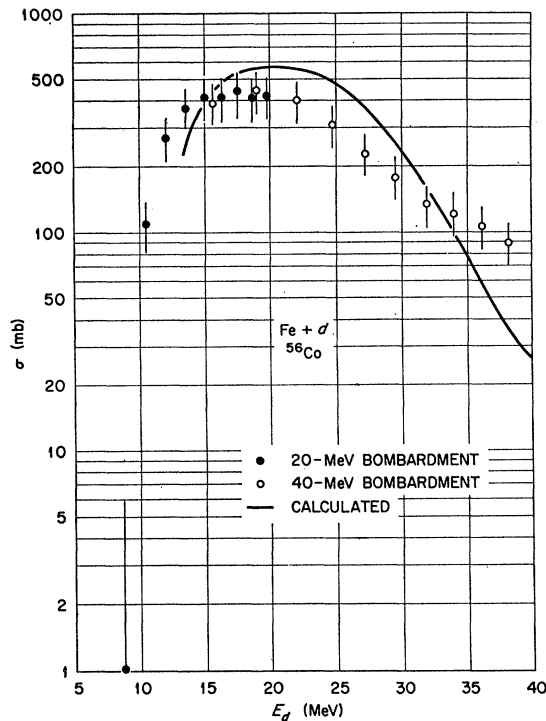


FIG. 5. Calculated excitation function for production of  $^{56}\text{Co}$  compared with the experimental data. The curve predicted by the theory (Ref. 14) was obtained for  $r_0=1.7$  F and  $a=4.0$ . The errors shown for the data points include uncertainties in absolute normalization.

the observed yield of  $^{57}\text{Co}$  was negligible; this is consistent with a Coulomb barrier of  $\sim 5$  MeV for the entrance channel. At the peaks of the respective excitation functions the cross sections are about equal, while the cross section at the peak of the part of the excitation function for  $^{56}\text{Co}$  due to  $^{56}\text{Fe}(d, 3n)$  is  $\sim$  a factor of 7 lower.

The low-energy peak of the  $^{56}\text{Co}$  curve, below the  $^{56}\text{Fe}(d, 3n)$  threshold, is due principally to the  $^{54}\text{Fe}(d, n)$  reaction. The  $Q$  value for this reaction is  $+2.9$  MeV. Thus the occurrence of a peak at  $\sim 7.5$  MeV is due to the Coulomb barrier for the entrance channel. When the cross section at the peak is divided by the isotopic abundance of  $^{54}\text{Fe}$  the cross section for the  $^{54}\text{Fe}(d, n)$  reaction is  $\sim 40\%$  lower than that observed for  $^{56}\text{Fe}(d, n)$ , i.e., the peak of the  $^{57}\text{Co}$  curve. A careful examination of possible experimental errors has convinced us that the  $^{54}\text{Fe}(d, n)$  cross section is lower than the  $^{56}\text{Fe}(d, n)$  cross section. The  $^{54}\text{Fe}$  nucleus contains 28 neutrons and therefore is considered to be a weakly closed neutron shell nucleus. While  $(d, n)$  reactions do not change the neutron number of the target nucleus the presence of the closed neutron shell may influence the emission of neutrons from the compound nucleus.

The  $^{56}\text{Fe}(d, 3n)$  reaction also results in a residual nucleus with 28 neutrons. The proximity of the closed neutron shell is a possible explanation for the low yield of  $^{56}\text{Fe}(d, 3n)$  compared with  $^{56}\text{Fe}(d, n)$  and  $(d, 2n)$  reactions. The part of the  $^{55}\text{Co}$  curve due to  $^{54}\text{Fe}(d, n)$  reaction, when corrected for isotopic abundance of  $^{54}\text{Fe}$ , yields a cross section of  $\sim 260$  mb at the peak of the excitation function. This is  $\sim 4$  times as large as the cross section at the peak of the excitation function, for the  $^{56}\text{Fe}(d, 3n)$  reaction. In both cases, the residual nucleus is the same. This is probably a better comparison of the relative cross sections for  $(d, n)$  and  $(d, 3n)$  than the relative yields of  $^{56}\text{Fe}(d, n)$  and  $^{56}\text{Fe}(d, 3n)$  reactions.

All of the measured excitation functions were compared with those predicted by a compound nucleus evaporation theory.<sup>14</sup> A Monte Carlo code<sup>15</sup> written in FORTRAN and modified for the ORNL CDC-1604-A computer was used to perform the calculations. In the calculations two parameters were varied. One is the parameter  $a$  of the Weisskopf level density<sup>16</sup> formula

$$W(E) = C \exp[2(aE)^{1/2}].$$

In earlier work<sup>17,18</sup> the best agreement with experimental results was obtained for values of  $a$  between 3 and 5. In the present work two values of  $a$  were used,  $a=4.0$  and  $a=9.5$ ; the better agreement was generally obtained for the smaller value.

The second parameter varied in the calculations was the nuclear radius parameter  $r_0$ . Calculations were made for  $r_0=1.5$  F and  $r_0=1.7$  F. Thus, four sets of calculations were made for each nuclide. In Fig. 4 the four curves thus obtained for  $^{52}\text{Mn}$  are compared with the experimental data. The best agreement with the data is obtained with the calculated curve for which  $r_0=1.7$  F and  $a=4.0$ . In general, the better agreement was obtained for all nuclides with the larger value of the radius parameter. This was also observed in earlier studies of proton-induced reactions.<sup>17,18</sup>

In Fig. 5 the excitation function for  $^{56}\text{Co}$  that is predicted by the nuclear evaporation theory with the parameters  $r_0=1.7$  F and  $a=4.0$  is compared with the experimental data. The two excitation functions are in reasonable agreement both in the shapes and magnitudes. At energies above 30 MeV, the calculated curve drops more rapid than the experimental data. A possible explanation is that the contributions of direct reactions to the observed yields increase as the energy increases.

<sup>14</sup> I. Dostrovsky, Z. Fraenkel, and G. Friedlander, Phys. Rev. **116**, 683 (1959).

<sup>15</sup> P. C. Rogers, Ph.D. thesis, Massachusetts Institute of Technology, 1962 (unpublished).

<sup>16</sup> V. F. Weisskopf, Phys. Rev. **52**, 295 (1937).

<sup>17</sup> I. R. Williams and C. B. Fulmer, Phys. Rev. **154**, 1005 (1967).

<sup>18</sup> D. Sheffey, I. R. Williams, and C. B. Fulmer, Phys. Rev. **172**, 1094 (1968).